Tutorials and Reviews

International Journal of Bifurcation and Chaos, Vol. 8, No. 8 (1998) 1643–1655

THE CONTROL OF CHAOS: THEORETICAL SCHEMES AND EXPERIMENTAL REALIZATIONS

F. T. ARECCHI*, S. BOCCALETTI†, M. CIOFINI and R. MEUCCI
Istituto Nazionale di Ottica, I-50125 Florence, Italy
**Department of Physics, University of Firenze, I-50125 Florence, Italy*
†*Department of Physics and Applied Mathematics, Universidad de Navarra, E-31080, Pamplona, Spain*

C. GREBOGI
University of Maryland, College Park, USA

Received July 31, 1997; Revised November 28, 1997

Controlling chaos is a process wherein an unstable periodic orbit embedded in a chaotic attractor is stabilized by means of tiny perturbations of the system. These perturbations imply goal oriented feedback techniques which act either on the state variables of the system or on the control parameters. We review some theoretical schemes and experimental implementations for the control of chaos.

1. Introduction

Controlling chaos consists in perturbing a chaotic system in order to stabilize a given unstable periodic orbit (UPO) embedded in the chaotic attractor (CA). The UPO's constitute the skeleton of chaotic dynamics, which, indeed, can be seen as a continuous irregular jumping process among neighborhoods of different periodic behaviors [Auerbach *et al.*, 1987]. Thus, control of chaos implies the extraction of desired periodic motions out of a chaotic one, through the application of judiciously chosen small perturbations. The process allows to exploit a single dynamical system for the production of a large number of different periodic behaviors, with an extreme flexibility in switching from one to another, so that the single system can carry out different performances with different yields.

The aim of this paper is to summarize some theoretical and experimental implementations of the above concepts. It is important to point out that the body of literature on this topic is very wide, and that the methodologies described here are by no means the only ones valid. Nevertheless, we hope that the reading of this paper may help researchers in entering this field, and in getting their bearings among the different methods.

In Sec. 2 we report the first control method, which was proposed by Ott *et al.* [1990] (OGY) and which consists in slight readjustments of a control parameter each time the trajectory crosses the Poincaré section (PS). Since a generic UPO is mapped on the PS by an ordered sequence of crossing points, OGY is able to stabilize such a sequence whenever the chaotic trajectory visits closely a neighborhood of one of the saddle PS points. The time lapse for a natural passage of the flow within the fixed neighborhood (hence for switching on the control process) can be very large. To minimize such a waiting time, a technique of targeting has been also introduced [Shinbrot *et al.*, 1993].

Another technique to constrain a nonlinear system $\mathbf{x}(t)$ to follow a prescribed goal dynamics $\mathbf{g}(t)$ [Plapp & Huebler, 1990] is based upon the addition to the equation of motion $d\mathbf{x}/dt = \mathbf{F}(\mathbf{x})$ of a term $\mathbf{U}(t)$ chosen in such a way that $|\mathbf{x}(t) - \mathbf{g}(t)| \to 0$ as $t \to \infty$. Plapp and Huebler choose $\mathbf{U}(t) = d\mathbf{g}/dt - \mathbf{F}(\mathbf{g}(t))$. The method provides robust

solutions, but in general the perturbation **U** would not be a small portion of the unperturbed dynamics **F**.

In other papers the effects of periodic [Lima & Pettini, 1990; Braiman & Goldhirsch, 1991; Azevedo & Rezende, 1991] and stochastic [Fahy & Hamann, 1992] perturbations is explored in producing dramatic changes in the dynamics, which eventually may lead to the selection of some UPO, even though they cannot be considered in general as goal oriented. This parametric perturbation avenue is explored in several companion papers of this issue.

Section 3 presents a method based upon the continuous application of a delayed feedback term in order to force the dynamical evolution of the system toward the desired periodic dynamics whenever the system visits such a periodic behavior closely [Pyragas, 1992].

Section 4 describes a frequency-domain control technique called "washout filter" [Tesi *et al.*, 1996; Basso *et al.*, 1997], based upon the insertion of a selective filter within a feedback loop.

Section 5 introduces the method of adaptive recognition [Arecchi *et al.*, 1994] and control [Boccaletti & Arecchi, 1995, 1996] of chaos. The method has later been successfully applied to chaos synchronization [Boccaletti *et al.*, 1997a], targeting of chaos [Boccaletti *et al.*, 1997b], filtering noise from chaotic data sets [Boccaletti *et al.*, 1997c], and eventually to the quenching of defects in an infinite dimensional dynamical system [Boccaletti *et al.*, 1997d]. The technique consists of a first step wherein the unperturbed features of the dynamics are extracted, and in a second step in which perturbations are done for the control of desired periodic orbits.

In Sec. 6 we review a few implementations of control of chaos in several experimental situations. The first experimental application of OGY was the stabilization of periodic orbits of a chaotic gravitationally buckled, amorphous magnetoelastic ribbon [Ditto *et al.*, 1990]. OGY inspired an easily realizable experimental technique called OPF (occasional proportional feedback), and demonstrated in a chaotic diode oscillator [Hunt, 1991].

Many other experimental systems have provided successful examples of chaos control. We recall among the others the thermal convection loop [Singer *et al.*, 1991], the yttrium iron garnet oscillator [Azevedo & Rezende, 1991], the optical multimode solid-state laser [Roy *et al.*, 1992], the Belouzov–Zabotinsky chemical reaction [Peng *et al.*, 1991; Petrov *et al.*, 1993], the optical fiber laser [Bielawski *et al.*, 1993], the CO_2 laser with modulation of losses [Meucci *et al.*, 1994], and the lead-salt diode laser [Chin *et al.*, 1996].

Finally, we discuss the experimental implementations of the "washout filter" technique of Sec. 4. The method has provided successful experimental applications both on autonomous [Meucci *et al.*, 1997] and nonautonomous [Ciofini *et al.*, 1997] chaotic CO_2 laser systems.

2. The OGY Control of Chaos

In this section we summarize the OGY method for the control of chaos [Ott *et al.*, 1990]. Even though such method holds regardless of the number of positive Liapunov exponents, for simplicity, we refer to a continuous-time chaotic dynamical system in a three-dimensional phase space, thus with a single positive Liapunov exponent. This is ruled by the differential equation

$$\frac{d\mathbf{x}}{dt} = \mathbf{F}(\mathbf{x}, p)\,, \tag{1}$$

where $\mathbf{x}$ is a D dimensional vector ($D = 3$), and p is a control parameter that we assume to be accessible for adjustments. The goal is to temporally program such adjustments so as to achieve stabilization of some UPO embedded within the chaotic attractor. Furthermore, we imagine that the functional form of **F** is not known, but that experimental time series of some scalar component $z(t)$ can be measured. By means of time-delay coordinates, and selecting an embedding time T, it is possible to reconstruct a $M + 1$ dimensional embedding space containing the vectors of the form

$$\mathbf{X}(t) \equiv [z(t),\, z(t-T),\, z(t-2T), \ldots,\, z(t-MT)]\,.$$

If one is interested in periodic orbits, one shall use **X** to obtain a surface of section, wherein any continuous-time-periodic orbit emerges as a discrete-time orbit cycling through a finite set of points. The requirement is that the embedding space has as many dimensions as there are coordinates of the point ($M = D - 1$), so that our surface of section is, in the present case, a two-dimensional surface. Let us now suppose that the control parameter p can be varied in a small interval about some nominal value p_0 (in the following, and without loss of generality, we take $p_0 = 0$), ranging within the interval $p_* > p > -p_*$. Again, let us

suppose that the experimental measurement contains many points in the surface of section for $p = 0$. By denoting such points as $\xi_1, \xi_2, \xi_3, \ldots, \xi_k$, then ξ_n are in general the coordinates at the nth intersection of the surface by the orbit $\mathbf{X}(t)$. A common choice of the surface is $z(t - MT) =$ constant, so that $\xi_n \equiv [z(t_n), \ldots, z(t_n - (M-1)T)]$, $t = t_n$ denoting the instant of the nth intersection.

Finally, let us denote by $\xi = \xi_F \equiv 0$ a given fixed point, by λ_s and λ_u respectively the stable and unstable eigenvalues of the surface at ξ_F, by $\mathbf{e}_s$ and $\mathbf{e}_u$ the unit vectors of the corresponding experimentally determined eigenvectors. When a change in p from $p = 0$ to some other value $p = \overline{p}$ is done, then the fixed point coordinate will shift correspondingly from 0 to some nearby point $\xi_F(\overline{p})$. For small $\overline{p}$ the following approximation holds

$$\mathbf{G} \equiv \frac{\partial \xi_F(p)}{\partial p} \simeq \frac{1}{\overline{p}} \xi_F(\overline{p})$$

which allows an experimental estimate of $\mathbf{G}$. On the surface and near $\xi = 0$, we can describe the dynamics with the linear map

$$\xi_{n+1} - \xi_F(p) \simeq \mathbf{M} \cdot [\xi_n - \xi_F(p)]$$

where $\mathbf{M}$ is a 2×2 matrix. Using $\xi_F(p) \simeq p\mathbf{G}$, the above equation reads

$$\xi_{n+1} \simeq p_n \mathbf{G} + [\lambda_u \mathbf{e}_u \mathbf{f}_u + \lambda_s \mathbf{e}_s \mathbf{f}_s] \cdot [\xi_n - p_n \mathbf{G}] \quad (2)$$

where $\mathbf{f}_s$ and $\mathbf{f}_u$ are controvariant basis vectors defined by $\mathbf{f}_s \cdot \mathbf{e}_s = \mathbf{f}_u \cdot \mathbf{e}_u \equiv 1$, $\mathbf{f}_s \cdot \mathbf{e}_u = \mathbf{f}_u \cdot \mathbf{e}_s \equiv 0$. Let us assume ξ_n be located within a neighborhood of the desired fixed point. The control method consists in selecting p_n so as ξ_{n+1} be put onto the stable manifold of $\xi = 0$, which implies to select p_n so that $\mathbf{f}_u \cdot \xi_{n+1} = 0$. When ξ_{n+1} falls on the stable manifold of the desired fixed point, the parameter can be set again to $p = 0$, because, by subsequent natural evolution, the dynamics will approach the desired fixed point at a geometrical rate λ_s.

Dotting (2) with $\mathbf{f}_u$, we obtain

$$p_n = \frac{\lambda_u}{\lambda_u - 1} \frac{\mathbf{f}_u \cdot \xi_n}{\mathbf{f}_u \cdot \mathbf{G}}$$

which can be used provided the magnitude of the right-hand side be smaller than p_*. In the opposite case, p_n is set to 0. As a consequence, the perturbation is activated only when ξ_n is located within a narrow strip $|\xi_n^u| < \xi_*$, $\xi_n^u = \mathbf{f}_u \cdot \xi_n$ and $\xi_* = p_* |(1 - \lambda_u^{-1}) \mathbf{G} \cdot \mathbf{f}_u|$.

This way, a stable periodic orbit is obtained out of the chaotic evolution of the dynamics. As we mentioned, the control of chaos gives flexibility. By turning the small controlling perturbations off, one can switch the time asymptotic behavior from one periodic orbit to another. In some situations, where flexibility offered by the ability to do such switching is desirable, it may be advantageous to design the system so that it is chaotic. In other situations, where one is presented with a chaotic system, the method may allow one to eliminate chaos and achieve great improved behavior at relatively low cost. The OGY ideas can also be applied to stabilize a desired chaotic trajectory, which has potential applications to problems such as synchronization of chaotic systems [Lai & Grebogi, 1993], conversion of transient chaos into sustained chaos [Lai & Grebogi, 1994], communication with chaos [Hayes *et al.*, 1993, 1994; Rosa *et al.*, 1997; Bollt *et al.*, 1997], and selection of a desired phase [Nagai & Lai, 1995].

3. The Pyragas' Method

An alternative time-continuous method [Pyragas, 1992] considers a dynamical system ruled by a set of unknown ordinary differential equations, and having some scalar variable accessible for measurements. Furthermore, the system possesses at least one input accessible for external forcing. The above assumptions are met by the following model

$$\frac{dy}{dt} = P(y, \mathbf{x}) + F(t)\,; \quad \frac{d\mathbf{x}}{dt} = \mathbf{Q}(y, \mathbf{x}) \quad (3)$$

where y represents the output scalar variable, $\mathbf{x}$ the remaining hidden variables of the dynamical system, $F(t)$ is an input signal which disturbs the dynamical evolution of the variable y, and P and $\mathbf{Q}$ are two nonlinear functions.

Let us imagine that system (3) produces chaotic dynamics for $F = 0$. In general, a large number of the UPO's within a chaotic attractor can be obtained from a single scalar variable through the standard method of delay coordinates. Therefore, one can extract from the measured variable y various periodic signals of the form $y = y_i(t)$, $y_i(t + T_i) = y_i(t)$, where T_i represents the period of the ith unstable periodic orbit.

To achieve stabilization of the selected UPO, let us design an external feedback line which reinjects into the system the difference $D(t)$ between

the signals $y(t)$ and $y(t-\tau)$ as a control signal:

$$F(t) = K[y(t-\tau) - y(t)] \tag{4}$$

where the weight K has to provide a negative feedback ($K < 0$) and τ represents a time delay. Stabilization of the ith UPO is achieved when τ equals the period T_i.

The method can be extended by adding information on previous periods, that is, replacing (4) with [Bleich & Socolar, 1996]

$$F(t) = K\left(y(t) - (1-R)\sum_{k=1}^{\infty} R^{k-1} y(t-k\tau)\right), \tag{5}$$

with $0 < R < 1$ a suitable real parameter, and k integer.

Notice that use of the perturbations (4) or (5) transforms the Ordinary Differential Equation (3) to a Delay Differential Equation. This requires some warning. As a delayed dynamical system is richer than an instantaneous one, care should be put in stabilizing a true UPO of the original unperturbed system, rather than a spurious UPO introduced artificially by the delay.

4. The Washout Filter

Control of chaos can be achieved by negative feedback of suitable spectral components of a system variable [Meucci *et al.*, 1996; Tesi *et al.*, 1996; Basso *et al.*, 1997; Ciofini *et al.*, 1997]. The set up consists in a feedback loop wherein all unwanted frequencies present in the chaotic spectrum are transmitted as correction signals by means of a selective filter ("washout filter"). In this way, the system is allowed to oscillate at the only frequency which is not fed back, namely, that of the unstable orbit to be stabilized. This control scheme is very easy to be implemented, besides having the relevant advantage of being robust and fast.

Consider a dynamical system modeled by ordinary differential equations in the form

$$\begin{aligned} \dot{x}_1 &= F(x_1, x_2) \\ \dot{x}_2 &= G(x_1, x_2)\,, \end{aligned} \tag{6}$$

F and G being a linear and a nonlinear function, respectively. The forthcoming considerations still hold in case the system is nonautonomous. Considering a stationary periodic regime where each variable can be approximated by $x_k \sim e^{st}$ ($s = i\omega$), let us introduce in the first equation a suitable negative feedback loop for x_1 through a "washout filter", characterized by a certain transfer function $C(s)$:

$$sx_1 = F(x_1, x_2) - x_1 C(s)\,.$$

The above equation can be also rewritten as

$$x_1 = \frac{F(x_1, x_2)}{s + C(s)}\,.$$

In order to stabilize a given orbit with pulsation Ω introducing a minimal perturbation, $C(s)$ should vanish for $\omega = 0$ and $\omega = \Omega$ (which implies that the feedback does not alter the fixed point and the limit cycle solutions of the unperturbed system). Moreover, depending on the route to chaos, it is useful to choose $C(s)$ so that it presents a maximum in correspondence to the frequency characteristic of the transition to chaos. Whenever the above conditions are fulfilled, the only frequency component which is not affected by the feedback is that of the cycle to be stabilized, while all the other components are sent back as a correction signal.

For example, in the case of the subharmonic route to chaos, the filter structure for stabilizing the period-1 (fundamental frequency $\tilde{f} = \Omega/2\pi$) orbit can be modeled as

$$C(s) = \beta \frac{s(s^2 + \Omega^2)}{\left(s^2 + \xi\Omega s + \dfrac{\Omega^2}{4}\right)(s + \mu\Omega)}$$

where $\xi = 0.4$, $\mu = 1.5$ and β is the gain factor. The amplitude and phase responses of the above transfer function are shown in Fig. 1 for $\tilde{f} = 110$ kHz; the maximum of $C(s)$ is set approximately at $\Omega/2$.

We add some remarks on the applications to real experimental conditions.

(i) This control scheme can be in principle very fast; indeed, the feedback loop can be entirely realized by analog electronics.

(ii) The control is also very robust since it is independent of parameter fluctuations.

(iii) Regarding the possibility of stabilizing more complex orbits (i.e. a period-2 orbit or a torus), one has just to design a different filter $C(s)$, with several zeroes corresponding to all the frequency components of the cycle to be stabilized.

(iv) The basic structure of Eqs. (6) (called Lur'e form) is peculiar of dynamical systems widely studied in the literature, such as the Chua circuit, the Rössler model and the Duffing oscillator [Genesio *et al.*, 1993].

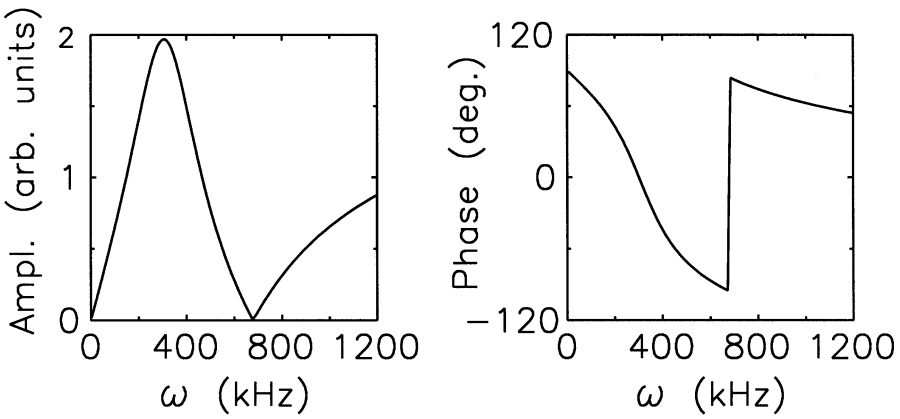

Fig. 1. Amplitude and phase response curves of the washout filter as a function of ω.

As a final consideration, we observe that this method presents several similarities with the time-delayed autosynchronization method [Pyragas, 1992; Basso *et al.*, 1997], despite the conceptual difference between these two techniques. In the frequency domain, the Pyragas' method can be seen as a negative feedback loop with a high-pass filter whose amplitude response goes to zero at the fundamental frequency Ω and for all its multiples $n\Omega$. In this way, the stabilized limit cycle is exactly the same as that of the unperturbed system since it contains all the harmonics, while the perturbation vanishes.

5. The Adaptive Algorithm

Let us consider a dissipative dynamics ruled by Eq. (1). The adaptive control technique consists in two successive steps, the first one, in which the unperturbed features of the dynamics are extracted [Arecchi *et al.*, 1994] and the periods of the UPO's are measured, and the second one whereby adaptive perturbations are applied in order to stabilize the selected UPO [Boccaletti & Arecchi, 1995, 1996].

We consider an observer "blind" to the main coordinate position x_i $(i = 1, \ldots, D)$ and interested only in its variation

$$\delta x_i(t_{n+1}) = x_i(t_{n+1}) - x_i(t_n)\,, \tag{7}$$

where $t_{n+1} - t_n = \tau_n$ is the nth adjustable interval, to be specified. In order to assign τ_{n+1} we consider the local variation rate

$$\lambda_i(t_{n+1}) = \frac{1}{\tau_n} \ln \left| \frac{\delta x_i(t_{n+1})}{\delta x_i(t_n)} \right| . \tag{8}$$

Here τ_{n+1} is the minimum of all $\tau_{n+1}^{(i)}$ corresponding to the different i, and defined by the rule

$$\tau_{n+1}^{(i)} = \tau_n^{(i)}(1 - \tanh(\sigma\lambda_i(t_{n+1})))\,. \tag{9}$$

Equation (9) arises from the following considerations. To obtain a sequence of geometrically regular δx_i, we shrink (stretch) the time intervals whenever the actual value of δx_i is larger (smaller) than the previously observed one. The hyperbolic tangent function maps the whole range of $\sigma\lambda_i$ into the interval $(-1, +1)$. The constant σ, strictly positive, is chosen in such a way as to forbid $\tau_n^{(i)}$ from going to zero. It may be taken as an *a priori* sensitivity, however, a more sensible assignment would consist in fixing σ by a moving average procedure, looking at the unbiased dynamical evolution for a while and then taking a σ value smaller than the reciprocal of the maximal λ recorded in that time span. Notice that a moving sensitivity is mandatory whenever the adaptive recognition is specialized to the measurement of a periodic orbit [Arecchi *et al.*, 1994].

We thus obtain a sequence of observation times starting from t_0

$$t_0, t_1 = t_0 + \tilde{\tau}\,,\ t_2 = t_1 + \tau_1, \ldots,\ t_{n+1} = t_n + \tau_n, \ldots \tag{10}$$

corresponding to which the variations of $\delta x_i(t_n)$ can be reduced below a preassigned value.

The observations performed at these times provide a "regularized" window, and the time sequence (10) now includes the chaotic information which was in the original geometric sequence $\mathbf{x}(t)$. The sequence (10) contains the relevant information on the dynamics, and we can characterize chaos as

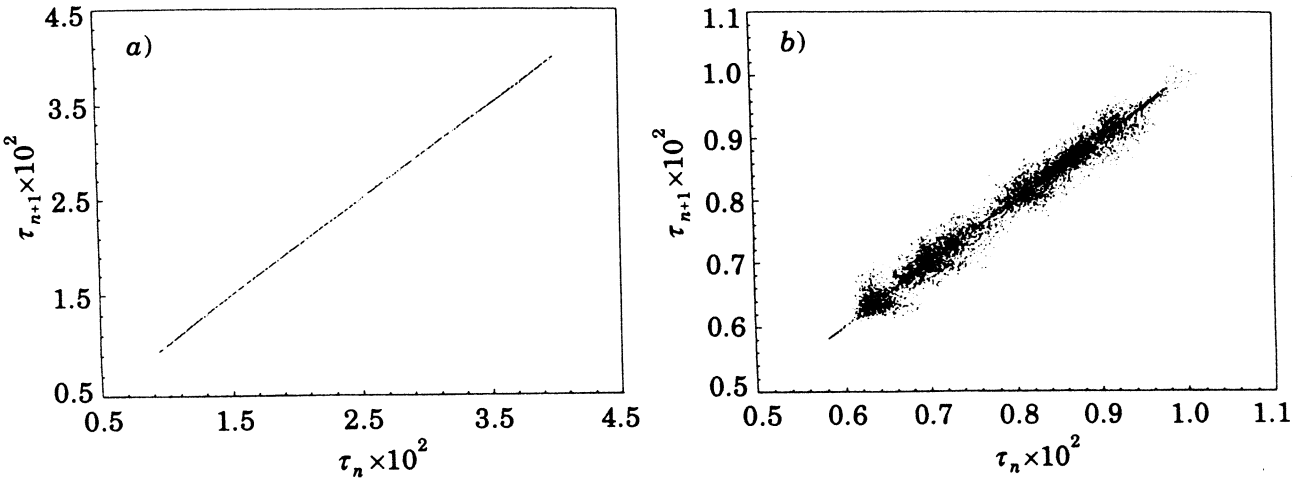

Fig. 2. Return maps τ_{n+1} versus τ_n for (a) Ro4 and (b) Ro4 with an additional 1% white noise. Initial conditions: $x(0) = -20$, $y(0) = z(0) = 0$, $w(0) = 15$. $g = 0.000048$.

follows. Since in Eq. (9) $|\sigma\lambda_i| \ll 1$, then two successive τ_n must be strongly correlated. As a result, even though the set of τ_n may be spread over a rather wide support, the return map τ_{n+1} versus τ_n must cluster along the diagonal. The residual deviations, averaged over many successive n's, provide the decorrelation trend, and hence yield an accurate assignment of the maximum Liapunov exponent. However, presence of large deviations from the diagonal denotes an uncorrelated perturbation. This may be some additive noise, which eventually can be filtered out, thus extracting the deterministic dynamics [Boccaletti *et al.*, 1997c].

In the following we will summarize the application of such a method to the Roessler four-dimensional (Ro4) model [Roessler, 1979] for a vector state $\mathbf{x} \equiv (x_1, x_2, x_3, x_4)$. For particular initial conditions ($x_1(0) = -20$, $x_2(0) = x_3(0) = 0$, $x_4(0) = 15$) and control parameters, Ro4 undergoes a hyperchaotic dynamics with two positive Liapunov exponents.

Figure 2 reports the return map of the τ_n for Ro4 and for Ro4 with 1% noise.

Since we are interested in stabilizing periodic dynamics, we need to extract the periods of UPO's embedded within the CA. For this purpose, instead of considering the single step map, we construct the maps τ_{n+k} versus τ_n, $k = 1, 2, \ldots$ and we plot the r.m.s. $\eta(k)$ of the point distribution around the diagonal of such maps as functions of the step interval k. For chaotic dynamics, temporal selfcorrelation lasts only for a finite time, hence one should expect to obtain a monotonically increasing function $\eta(k)$. In fact, the chaotic dynamics steers the phase-space trajectory toward neighborhoods of different UPO's. As the trajectory gets close to an UPO of period T_j, temporal selfcorrelation is rebuilt after T_j and the distribution of τ includes windows of correlated values appearing as minima of η versus k around $k_j = T_j/\langle\tau\rangle$, $\langle\tau\rangle$ being the average of the τ distribution.

To give an exemple, we report in Fig. 3 the η-k plot for Ro4, from which one can extract the different UPO's periods looking to the minima of the η curve. In fact, during the observation, the

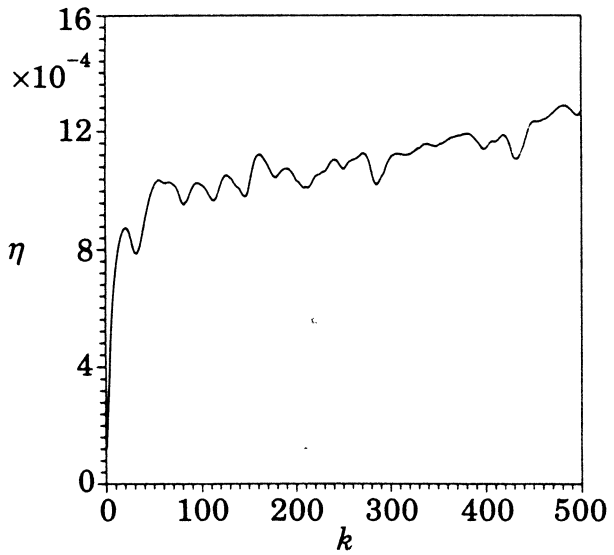

Fig. 3. η-k plot for Ro4 attractor. Initial conditions and control parameters as in the text. The recognition task has been performed with $g = 0.01$. Vertical axis has to be multiplied for 10^{-4}.

time intervals are changing, and a more rigorous determination of the period is provided by minimizing a suitable cost function in the vicinity of each minimum of the η curve [Boccaletti & Arecchi, 1995].

Once the periods T_j ($j = 1, 2, \ldots$) of the UPO's have been measured, stabilization of each one can be achieved when the system naturally visits closely phase space neighborhoods of that UPO. For a nonauthonomous system, a period T may correspond to many degenerate UPO's. In this case, selection of the desired one can be achieved by the study of the topology of all UPO's corresponding to the same period and by switching-on the control task when the system is shadowing the selected UPO. Several topological approaches to the UPO's detection have been developed [Cvitanovic *et al.*, 1988; Gunaratne *et al.*, 1989; Mindlin *et al.*, 1990; Tufillaro *et al.*, 1990].

The control procedure is done by use of the following modified algorithm. At each new observation time $t_{n+1} = t_n + \tau_n$ and for each component i of the dynamics, instead of Eq. (7), we evaluate the differences between actual and desired values

$$\delta x_i(t_{n+1}) = x_i(t_{n+1}) - x_i(t_{n+1} - T_j)\,, \qquad (11)$$

and the local variation rates λ's now read

$$\lambda_i(t_{n+1}) = \frac{1}{\tau_n} \log \left| \frac{x_i(t_{n+1}) - x_i(t_{n+1} - T_j)}{x_i(t_n) - x_i(t_n - T_j)} \right| . \qquad (12)$$

We keep Eq. (9) and the choice of the minimum for the updating process of τ's. Defining $\mathbf{U}(t)$ as the vector with ith component (constant over each observation time interval) given by

$$U_i(t_{n+1}) = \frac{1}{\tau_{n+1}} (x_i(t_{n+1} - T_j) - x_i(t_{n+1}))\,, \quad (13)$$

we add such a vector to the evolution equation, which then becomes

$$\frac{d\mathbf{x}}{dt} = \mathbf{F}(x, p) + \mathbf{U}(t)\,. \qquad (14)$$

Notice that the λ's given by Eq. (12) track the rate of separation of the actual trajectory from the desired one. Indeed, λ negative means that locally the true orbit is collapsing into the desired one and hence the actual dynamics is shadowing the desired UPO, while λ positive implies that the actual trajectory is locally diverging away from the desired one and control has to be performed in order to constrain the orbit to shadow the desired UPO.

As a consequence, contraction or expansion of τ's now reflects the need to perturb the dynamics more or less robustly in order to stabilize the desired UPO. This appears as a weight to the correction of Eq. (13), which, once a given T_j has been chosen by the operator, is selected by the same adaptive dynamics.

Once again, the introduced adaptive weighting procedure in Eq. (13) assures the effectiveness of the

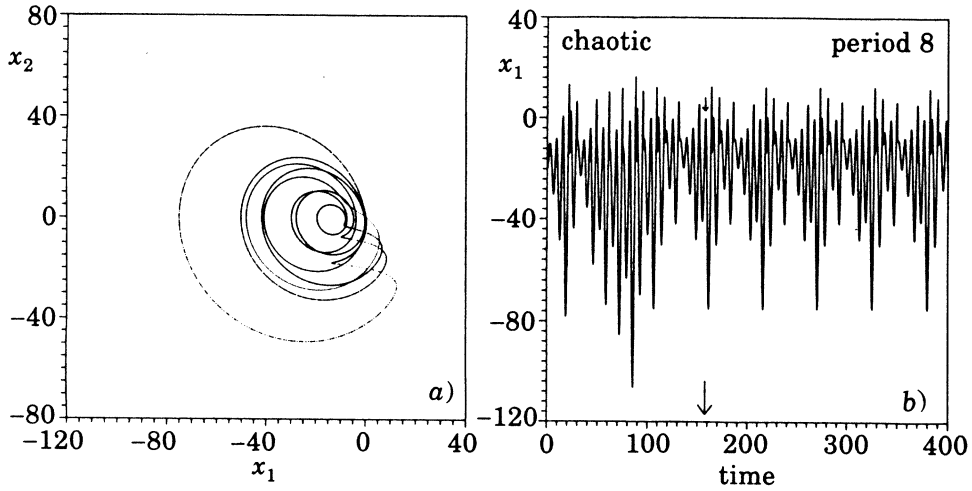

Fig. 4. (a) (x_1, x_2) projection of the phase space portrait for the controlled period-8 of Ro4 attractor. Control task has been performed with period-8 extracted from Fig. 3 and $g = 10^{-5}$. (b) Time evolution of the first component x_1 of Ro4 before and after control. Arrows indicate the instant at which control task begins.

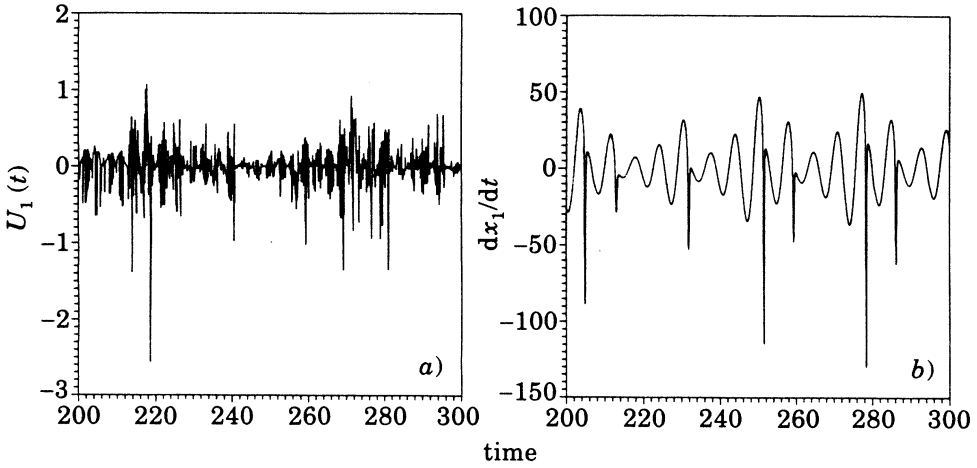

Fig. 5. (a) Temporal evolution of the first component of the additive controlling term U_1 during the control of period-8 of Ro4 and (b) temporal evolution of the uncontrolled dx_1/dt. The adaptive correction term is between two and three orders of magnitude smaller than the natural evolution of the dynamics. Same stipulation for controlling task as mentioned in the caption of Fig. 4.

method (perturbation is larger or smaller whenever it has to be) as well as the fact that the additive term **U** is much smaller than the unperturbed dynamics **F**.

In Fig. 4 we show the control of period-8 of Ro4.

Figure 5 reports the perturbation $U_1(t)$ and the unperturbed dynamics G_1 for the Ro4 model during the control task of period-8, in order to show that the former is between two and three orders of magnitude smaller than the latter as expected by the above discussion.

Notice that the limit $\sigma = 0$ of the above algorithm recovers [Pyragas, 1992]. Choosing $\sigma \neq 0$ implies an adaptive nature of the forcing term [Eq. (13)] which is inversely proportional to the time intervals and hence is weighted by the information extracted from the dynamics itself.

Applications of this method have been already reported in the introductory section.

6. Review of Some Control Experiments

The OGY method described in Sec. 2 has found applications in several experimental situations. As an example, we herewith report the first experimental realization of chaos control which was done in 1990 by Ditto *et al.* [1990].

In this case, the theoretical background of Sec. 2 has been applied to an experimental system consisting of a gravitationally buckled, amorphous magnetoelastic ribbon. The ribbon exhibits large reversible changes of its Young's modulus when small magnetic fields are applied. It is clamped at the base, yielding a free vertical length greater than the Euler buckling length, thus providing an initial buckling configuration. The ribbon is placed within three mutually orthogonal pairs of Helmoltz coils, allowing to compensate for the Earth's magnetic field. Finally, a uniform vertical magnetic field is applied along the ribbon. In this configuration, the Young's modulus of the ribbon is varied due to the applied vertical magnetic field which has the form $H = H_{\rm dc} + H_{\rm ac}\cos(2\pi f t)$. Both amplitudes have been set typically in the range 0.1–2.5 Oe. A measurement of the curvature of the ribbon near the base is provided by a sensor.

The experimental data consist in time series voltages $V(t)$ acquired from the output of the sensor and sampled at the drive period of the ac magnetic field (i.e. at times $t_n = n/f$). The sampled voltages are considered as iterates of the map $X_n = V(t_n)$ and the control theory in Sec. 2 is applied, taking as control parameter the amplitude of the continuous component of the magnetic field $H_{\rm dc}$. Selecting $H_{\rm ac}$, $H_{\rm dc}$ and f so as to produce chaotic dynamics, control of period-1 UPO is achieved for over 200 000 iterates (approximately 64 hours) with maximum perturbation of about 1% of the unperturbed control parameter. With the same setup, control of one of the period-2 UPO is also achieved.

A modification of the OGY method, called occasional proportional feedback (OPF) has been used to stabilize unstable orbits in a chemical system

[Peng *et al.*, 1991, Petrov *et al.*, 1993] and in a diode resonator [Hunt, 1991]. This technique consists in feeding back deviations of the chaotic variable within a specified window from a reference point to perturb a control parameter. The chemical experiment deals with the Belousov–Zhabotinsky reaction carried out in a continuous-flow stirred-tank reactor. The flow rate μ of the reactants into the tank ultimately determines whether the system shows steady state, periodic and chaotic behaviors. The control algorithm takes advantage of the predictable evolution of the chaotic system in the vicinity of a fixed point in the next-amplitude return map of a suitable variable A (dimensionless concentration). The position of the period-1 fixed point is given by the intersection of the map with the bisectrix, where $A_{n+1} = A_n = A_s$. The map can be shifted to target the fixed point by applying a perturbation to the bifurcation parameter μ according to the difference between the system state and the fixed point

$$\Delta\mu = \frac{A_n - A_s}{g}$$

where g is a suitable constant. In an analogous manner (changing A_s and g) period-2 and period-4 unstable orbits have been stabilized.

The electronic experiment consists of a *p-n* junction rectifier in series with an inductor. The system exhibits the period-doubling route to chaos when driven with an increasing sinusoidal voltage. The current through the diode provides a convenient chaotic variable; if the peak current I_n falls within a given window, the driving voltage is amplitude modulated with a signal proportional to the difference between I_n and the center of the window. By changing the level and the width of the window, or the gain of the feedback signal, several unstable orbits are stabilized, up to the period-23.

The OPF has been also applied by Roy *et al.* [1992] to an autonomously chaotic multimode laser, that is, a high dimensional system for which the chaotic attractor is not characterized by a low-dimensional map. The experimental setup consists of a diode-laser-pumped solid state Nd-doped yttrium aluminum garnet (Nd:YAG) laser containing a KTP doubling crystal. The source of chaotic behavior in this laser is the coupling of the longitudinal modes through the nonlinear process of sum-frequency generation. This process destabilizes the relaxation oscillations which are normally damped in a system without the intracavity KTP crystal. The total laser output intensity is sampled within a window of selected offset and width, and a signal proportional to the deviation from the center of the window is applied to perturb the injection current of the pumping laser diodes. With this configuration period-1, -4 and -9 limit cycles have been successfully stabilized with relative perturbation amplitude less than 10%.

The control scheme proposed by Pyragas (discussed in Sec. 3) has been first experimentally demonstrated in an electronic circuit [Gauthier *et al.*, 1994] and in a modulated laser [Bielawski *et al.*, 1994]. In the first experiment, the setup is similar to that reported by Hunt, the only difference being that the resonator has been modified to operate at higher frequency (10 MHz). The control is derived by directing half of the voltage signal (proportional to the resonator current) directly into one input of a summing amplifier, while the other half, delayed and inverted, is sent to the second input. The delay line consists of a cable with length precisely adjusted so that it provides a delay τ corresponding to the period of the desired UPO. The control signal is reinjected into the resonator as an additive perturbation of the driving voltage. In this way, a close reproduction of the control Eq. (4) is achieved, allowing stabilization and tracking of period-1, -2 and -4 unstable limit cycles.

The second experiment deals with a CO_2 laser with cavity loss modulation, obtained by driving an intracavity electro-optic crystal with an external sinusoidal voltage. In this case, the chaotic variable is the infrared (10 μm) laser light, monitored by a fast photovoltaic detector. The detector voltage is used to modulate a laser diode emitting at 845 nm so that a time delayed voltage can be obtained by propagating the laser diode light in a long fiber and detecting it at the end. Finally, the difference between the CO_2 laser intensity and its delayed version is added to the modulation signal after suitable amplification. With such a configuration the unstable period-1 orbit is stabilized and tracked along a wide range in the bifurcation diagram.

The experimental implementation of the control scheme based on the washout filter has been tested in the chaotic regimes of both a nonautonomous system [Meucci *et al.*, 1996; Ciofini *et al.*, 1997] (a CO_2 laser with externally modulated losses) and of an autonomous system [Meucci *et al.*, 1997] (a CO_2 laser with intensity feedback), obtaining stabilization and tracking of different unstable periodic orbits, with perturbation amplitudes of the order of few percent.

The experimental setup consists of a single mode CO_2 laser with an intracavity electro-optic crystal which can be driven by an external voltage $V(t)$ to modulate the cavity losses k. In the nonautonomous case, the driving voltage $V(t)$ is a sinusoidal signal, so that the cavity loss parameter k becomes: $k = k_0[1+m\,\sin(2\pi f t)]$, where $f = 110$ kHz is the modulation frequency and the modulation depth m, proportional to the amplitude of $V(t)$, is the control parameter. By increasing m the system undergoes the transition to chaos through a sequence of subharmonic bifurcations. The period-1 orbit is stable up to $m = 0.1$, and a further increase of m drives the system to period-2 and period-4 orbits, followed by the first chaotic region and, finally, by a period-3 stable solution. The control was implemented with a negative feedback loop where the laser intensity, revealed by a fast detector, is first filtered and then subtracted from $V(t)$. The characteristic curves in Fig. 1 have been closely reproduced by a two-stage passive filter (a band-pass stage combined with a Notch stage) entirely realized by analog circuitry (Fig. 6).

Figure 7 reports the experiment. Figure 7(a) is the chaotic laser oscillations ($m = 0.18$) observed

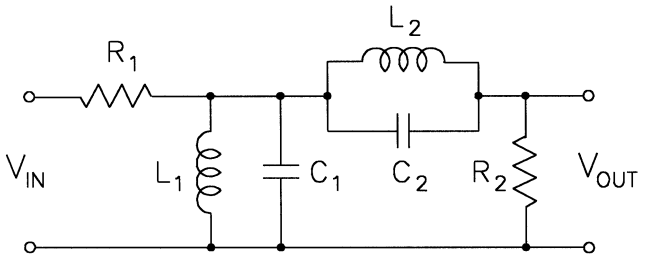

Fig. 6. Electronic scheme of the washout filter: $R_1 = 1$ kΩ, $L_1 = 6.5$ mH, $C_1 = 0.1$ nF, $R_2 = 6.7$ kΩ, $L_2 = 12.4$ mH and $C_2 = 0.2$ nF.

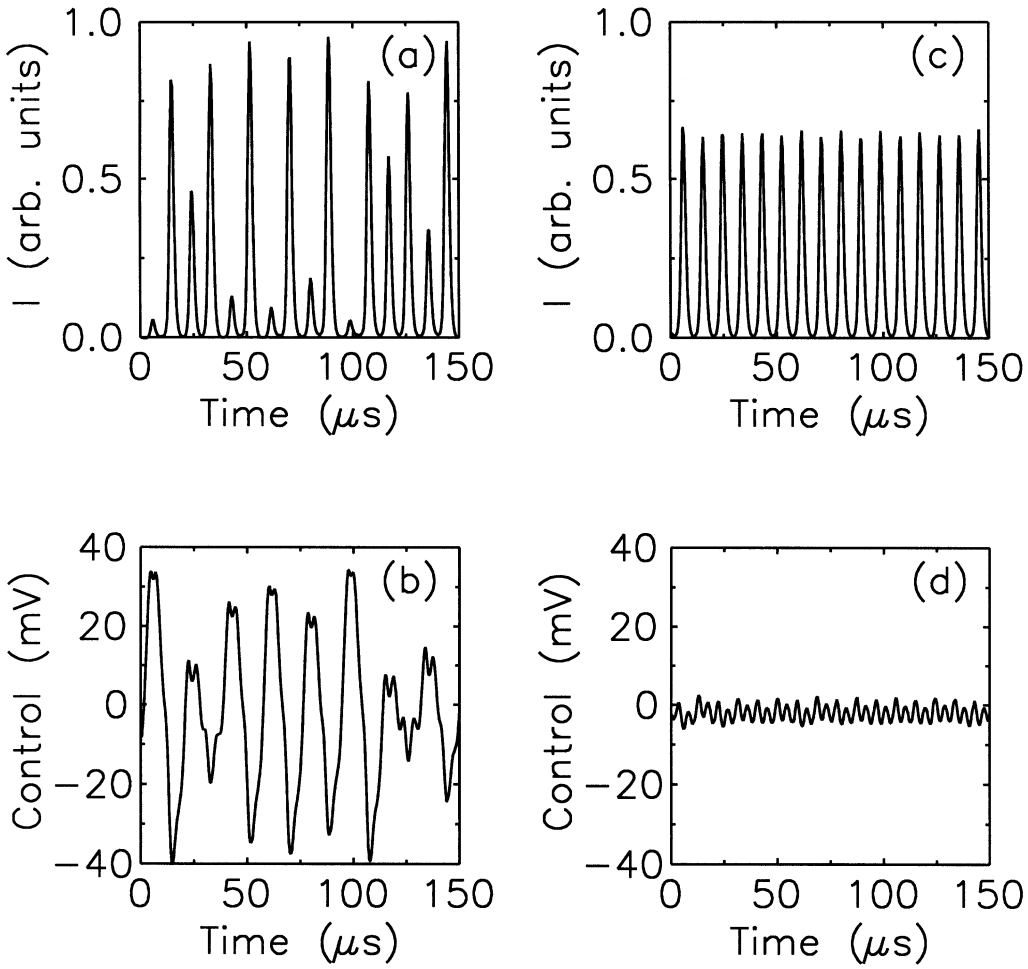

Fig. 7. Experimental results: (a) chaotic laser intensity without control and (b) corresponding control signal; (c) and (d) represent the same signals as (a) and (b), respectively, but in the case of activated control.

with open control loop, while Fig. 7(b) is the corresponding control signal. The same signals are reported in Figs. 7(c) and 7(d), respectively, but in the case of a closed control loop. The control signal amplitude of Fig. 7(b) provides a 1.25% perturbation of the driving signal. This result confirms that the method allows stabilization of unstable orbits slightly different from those embedded in the unperturbed system.

Following the above criteria, a second filter has been prepared allowing stabilization of the period-2 limit cycle, and both filters have been used to track the corresponding trajectory along the whole bifurcation diagram. The unperturbed bifurcation diagram has been measured by increasing the control parameter m at fixed steps, and processing the laser intensity in order to extract the maxima (Fig. 8). The same measurements have been repeated after the insertion of the feedback loops with the two filters. Figures 8(a) and 8(b) show the superposition of the unperturbed bifurcation diagram (dots) with the tracked period-1 and period-2 orbits (circles), respectively. In both cases the tracking has been achieved without any readjustment of the gain of the feedback loop over the whole explored range, and with relative perturbation amplitudes less than 3%.

In a different experiment, the control has been tested on a CO_2 laser made chaotic by an intensity feedback. In this case the system is autonomous, since the modulator voltage $V(t)$ carries information on the output intensity. Indeed it is obtained by detecting the laser output and then amplifying such a signal. The equation for $V(t)$ is

$$\dot{V} = -\beta \left(V - B + \frac{RI}{1 + \alpha I} \right)$$

where β is the damping rate of the feedback loop, I is the laser intensity, B a bias voltage acting as the control parameter and R the total gain of the loop (the term αI represents the saturation of the detection apparatus).

Starting from constant laser output and increasing B, the system passes to a limit cycle through a Hopf bifurcation, and then it reaches the chaotic region after a subharmonic cascade. The spectral analysis of the chaotic signal for $B = 360$ V shows the presence of a peak at $\tilde{f} = 22$ kHz, remnant of the Hopf bifurcation. This property suggests to prepare a suitable washout filter with zero amplitude in correspondence of $\tilde{f}$. Figure 9 shows the three-dimensional reconstruction of the chaotic attractor and the stabilized period-1 orbit obtained with a relative perturbation of about 7%.

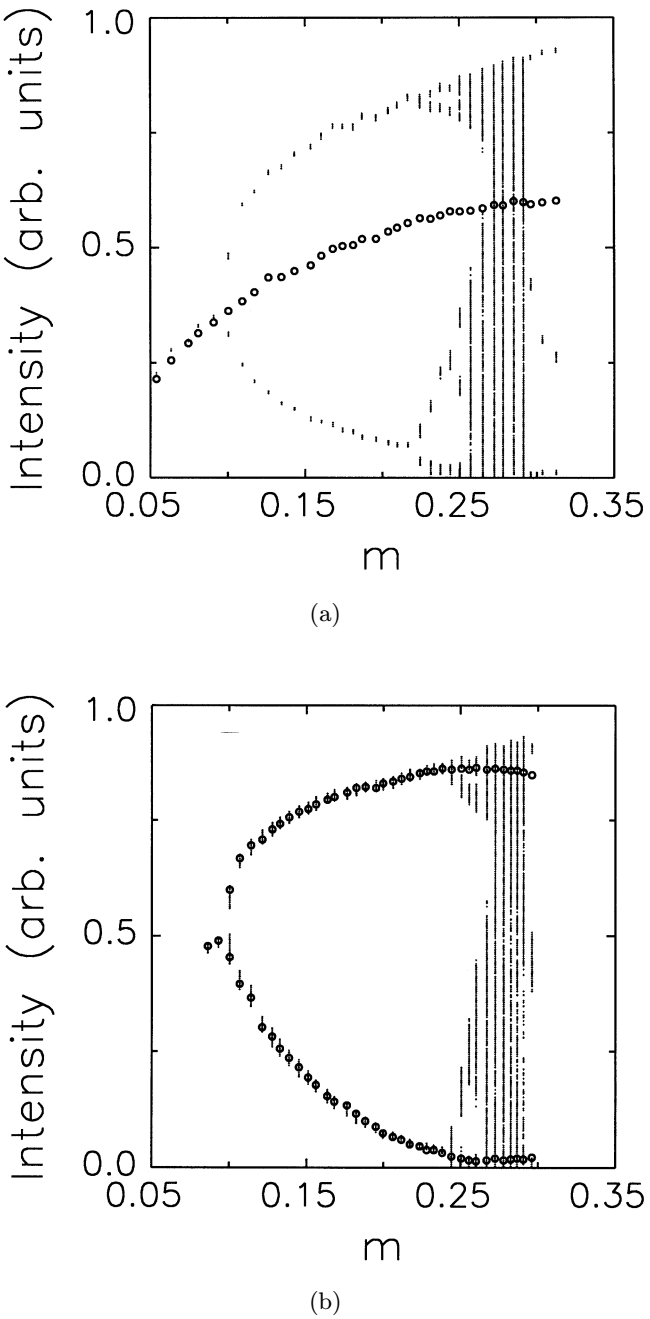

Fig. 8. Experimental results of the tracking of (a) period-1 unstable orbit and (b) period-2 unstable orbit. Circles and points: maxima in the laser output signal with and without the control loop, respectively.

All the experimental results can be adequately reproduced by numerical integration of a CO_2 laser model based on rate equations for the intensity and for the populations of the resonant levels coupled by collisions with the rotational manifolds.

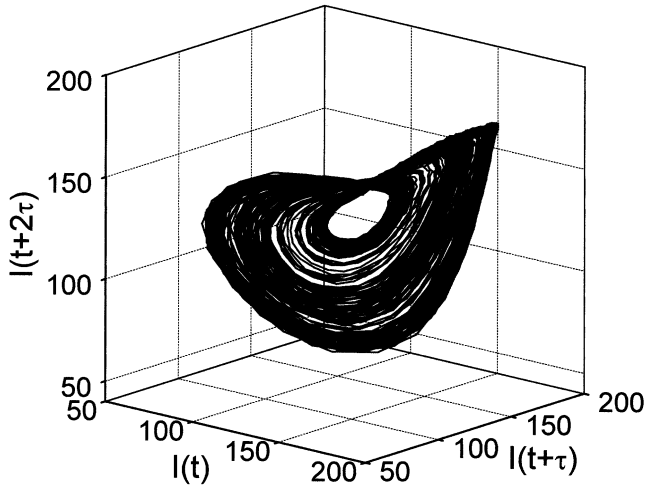

(a)

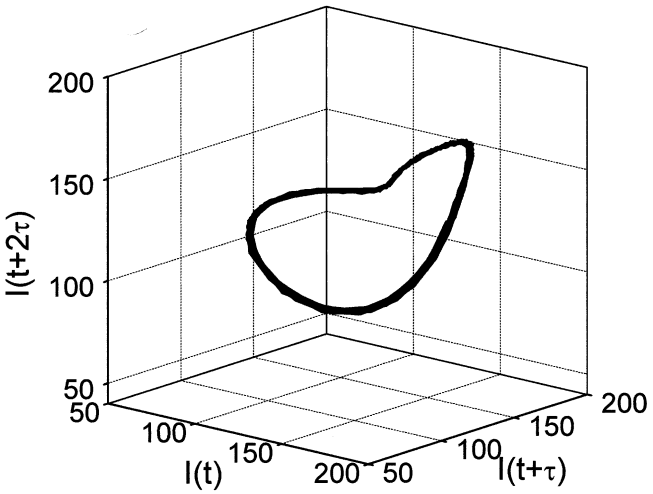

(b)

Fig. 9. (a) Three-dimensional reconstruction of the chaotic attractor and (b) stabilized period-1 orbit.

References

Arecchi, F. T., Basti, G., Boccaletti, S. & Perrone, A. L. [1994] "Adaptive recognition of a chaotic dynamics," *Europhys. Lett.* **26**, 327–332.

Auerbach, D., Cvitanovic, P., Eckmann, J.-P., Gunaratne, G. & Procaccia, I. [1987] "Exploring chaotic motion through periodic orbits," *Phys. Rev. Lett.* **58**, 2387–2390.

Azevedo, A. & Rezende, S. M. [1991] "Controlling chaos in spin-wave instabilities," *Phys. Rev. Lett.* **66**, 1342–1345.

Basso, M., Genesio, R. & Tesi, A. [1997] "Controlling chaos in a CO_2 laser," *Proc. 4th European Control Conference, Bruxelles.*

Bielawski, S., Derozier, D. & Glorieux, P. [1993] "Experimental characterization of unstable periodic orbits by controlling chaos," *Phys. Rev.* **A47**, R2492–2495.

Bielawski, S., Derozier, D. & Glorieux, P. [1994] "Controlling unstable periodic orbits by a delayed continuous feedback," *Phys. Rev.* **E49**, R971–974.

Bleich, M. E. & Socolar, J. E. S. [1996] "Stability of periodic orbits controlled by time-delay feedback," *Phys. Lett.* **A210**, 87–94.

Boccaletti, S. & Arecchi, F. T. [1995] "Adaptive control of chaos," *Europhys. Lett.* **31**, 127–132.

Boccaletti, S. & Arecchi, F. T. [1996] "Adaptive recognition and control of chaos," *Physica* **D96**, 9–16.

Boccaletti, S., Farini, A. & Arecchi, F. T. [1997a] "Adaptive synchronization of chaos for secure communication," *Phys. Rev.* **E55**, 4979–4982.

Boccaletti, S., Farini, A., Kostelich, E. J. & Arecchi, F. T. [1997b] "Adaptive targeting of chaos," *Phys. Rev.* **E55**, R4845–4848.

Boccaletti, S., Giaquinta, A. & Arecchi, F. T. [1997c] "Adaptive recognition and filtering of noise using wavelets," *Phys. Rev.* **E55**, 5393–5400.

Boccaletti, S., Maza, D., Mancini, H., Genesio, R. & Arecchi, F. T. [1997d] "Control of defects and spacelike structures in delayed dynamical systems," *Phys. Rev. Lett.* **79**, 5246–5249.

Bollt, E., Lai, Y. C. & Grebogi, C. [1997] "Coding, channel capacity and noise resistance in communication with chaos," *Phys. Rev. Lett.* **79**, 3787–3790.

Braiman, Y. & Goldhirsch, I. [1991] "Taming chaotic dynamics with weak periodic perturbations," *Phys. Rev. Lett.* **66**, 2545–2548.

Chin, G., Senesac, L. R., Blass, W. E. & Hillman, J. J. [1996] "Stabilizing lead-salt diode lasers: Understanding and controlling chaotic frequency emission," *Science* **274**, 1498–1501.

Ciofini, M., Labate, A. & Meucci, R. [1997] "Tracking unstable periodic orbits in a modulated laser," *Phys. Lett.* **A227**, 31–36.

Cvitanovic, P., Gunaratne, G. H. & Procaccia, I. [1988] "Topological and metric properties of Hénon-type strange attractors," *Phys. Rev.* **A38**, 1503–1520.

Ditto, W. L., Rauseo, S. N. & Spano, M. L. [1990] "Experimental control of chaos," *Phys. Rev. Lett.* **65**, 3211–3214.

Fahy, S. & Hamann, R. D. [1992] "Transition from chaotic to nonchaotic behavior in randomly driven systems," *Phys. Rev. Lett.* **69**, 761–764.

Gauthier, D. J., Sukow, D. W., Concannon, H. M. & Socolar, J. E. S. [1994] "Stabilizing unstable periodic orbits in a fast diode resonator using continuous time-delay autosynchronization," *Phys. Rev.* **E50**, 2343–2346.

Genesio, R., Tesi, A. & Villoresi, F. [1993] "A frequency approach for analyzing and controlling chaos in nonlinear circuits," *IEEE Trans. Circuits Syst. I: Fundamental Theor. Appl.* **40**, 819–828.

Gunaratne, G. H., Linsay, P. S. & Vinson, M. J. [1989] "Chaos beyond onset: A comparison of theory and experiment," *Phys. Rev. Lett.* **63**, 1–4.

Hayes, S., Grebogi, C. & Ott, E. [1993] "Communication with chaos," *Phys. Rev. Lett.* **70**, 3031–3034.

Hayes, S., Grebogi, C., Ott, E. & Mark, A. [1994] "Experimental control of chaos for communication," *Phys. Rev. Lett.* **73**, 1781–1784.

Hunt, E. R. [1991] "Stabilizing high-period orbits in a chaotic system: The diode resonator," *Phys. Rev. Lett.* **67**, 1953–1956.

Lai, Y. C. & Grebogi, C. [1993] "Synchronization of chaotic trajectories using control," *Phys. Rev.* **E47**, 2357–2360.

Lai, Y. C. & Grebogi, C. [1994] "Converting transient chaos into sustained chaos by feedback control," *Phys. Rev.* **E49**, 1094–1099.

Lima, R. & Pettini, M. [1990] "Suppression of chaos by resonant parametric perturbations," *Phys. Rev.* **A41**, 726–733.

Meucci, R., Gadomski, W., Ciofini, M. & Arecchi, F. T. [1994] "Experimental control of chaos by means of weak parametric perturbations," *Phys. Rev.* **E49**, R2528–2531.

Meucci, R., Ciofini, M. & Abbate, R. [1996] "Suppressing chaos in lasers by negative feedback," *Phys. Rev.* **E53**, R5537–5540.

Meucci, R., Labate, A. & Ciofini, M. [1997] "Controlling chaos by negative feedback of subharmonic components," *Phys. Rev.* **E56**, 2829–2834.

Mindlin, G. B., Hou, X.-J., Solari, H. G., Gilmore, R. & Tufillaro, N. B. [1990] "Classification of strange attractors by integers," *Phys. Rev. Lett.* **64**, 2350–2353.

Nagai, Y. & Lai, Y. C. [1995] "Selection of desirable chaotic phase using small feedback control," *Phys. Rev.* **E51**, 3842–3848.

Ott, E., Grebogi, C. & Yorke, J. A. [1990] "Controlling chaos," *Phys. Rev. Lett.* **64**, 1196–1199.

Peng, B., Petrov, V. & Showalter, K. [1991] "Controlling chemical chaos," *J. Phys. Chem.* **95**, 4957–4959.

Petrov, V., Gaspar, V., Masere, J. & Showalter, K. [1993] "Controlling chaos in the Belousov–Zhabotinsky reaction," *Nature* **361**, 240–242.

Plapp, B. B. & Huebler, A. W. [1990] "Nonlinear resonances and suppression of chaos in the rf-biased Josephson junction," *Phys. Rev. Lett.* **65**, 2302–2305.

Pyragas, K. [1992] "Continuous control of chaos by self-controlling feedback," *Phys. Lett.* **A170**, 421–428.

Roessler, O. E. [1979] "An equation for hyperchaos," *Phys. Lett.* **71A**, 155–157.

Rosa, E., Hayes, S. & Grebogi, C. [1997] "Noise filtering in communication with chaos," *Phys. Rev. Lett.* **78**, 1247–1250.

Roy, R., Murphy Jr., T. W., Maier, T. D., Gills, Z. & Hunt, E. R. [1992] "Dynamical control of a chaotic laser: Experimental stabilization of a globally coupled system," *Phys. Rev. Lett.* **68**, 1259–1262.

Shinbrot, T., Grebogi, C., Ott, E. & Yorke, J. A. [1993] "Using small perturbations to control chaos," *Nature* **363**, 411–417.

Singer, J., Wang, Y.-Z. & Bau, H. H. [1991] "Controlling a chaotic system," *Phys. Rev. Lett.* **66**, 1123–1126.

Tesi, A., Abed, E. H., Genesio, R. & Wang, O. H. [1996] "Harmonic balance analysis of period-doubling bifurcations with implications for control of nonlinear dynamics," *Automatica* **32**, 1255–1271.

Tufillaro, N. B., Solari, H. G. & Gilmore, R. [1990] "Relative rotation rates: Fingerprints for strange attractors," *Phys. Rev.* **A41**, R5717–R5720.